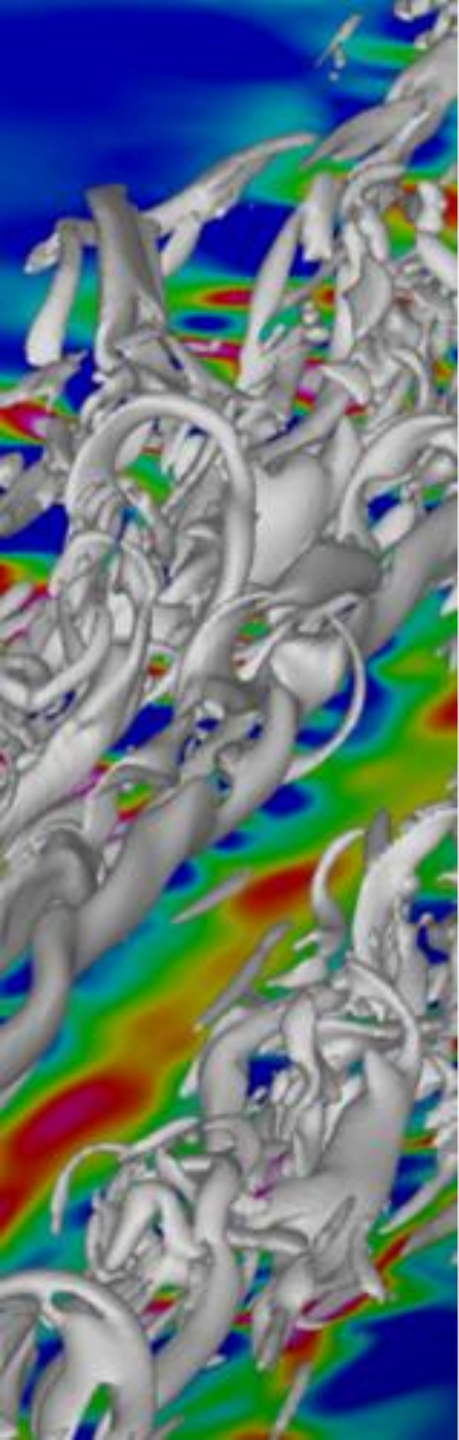

Prospects for High-Speed Flow Simulations

Graham V. Candler
Aerospace Engineering & Mechanics
University of Minnesota

Support from AFOSR and ASDR&E

Future Directions in CFD Research:
A Modeling & Simulation Conference

August 7, 2012

Today's Talk

- Motivating problems in high-speed flows
- An implicit method for aerothermodynamics / reacting flows
- A kinetic energy consistent, low-dissipation flux method
- Some examples

Transition in Ballistic Range at M = 3.5

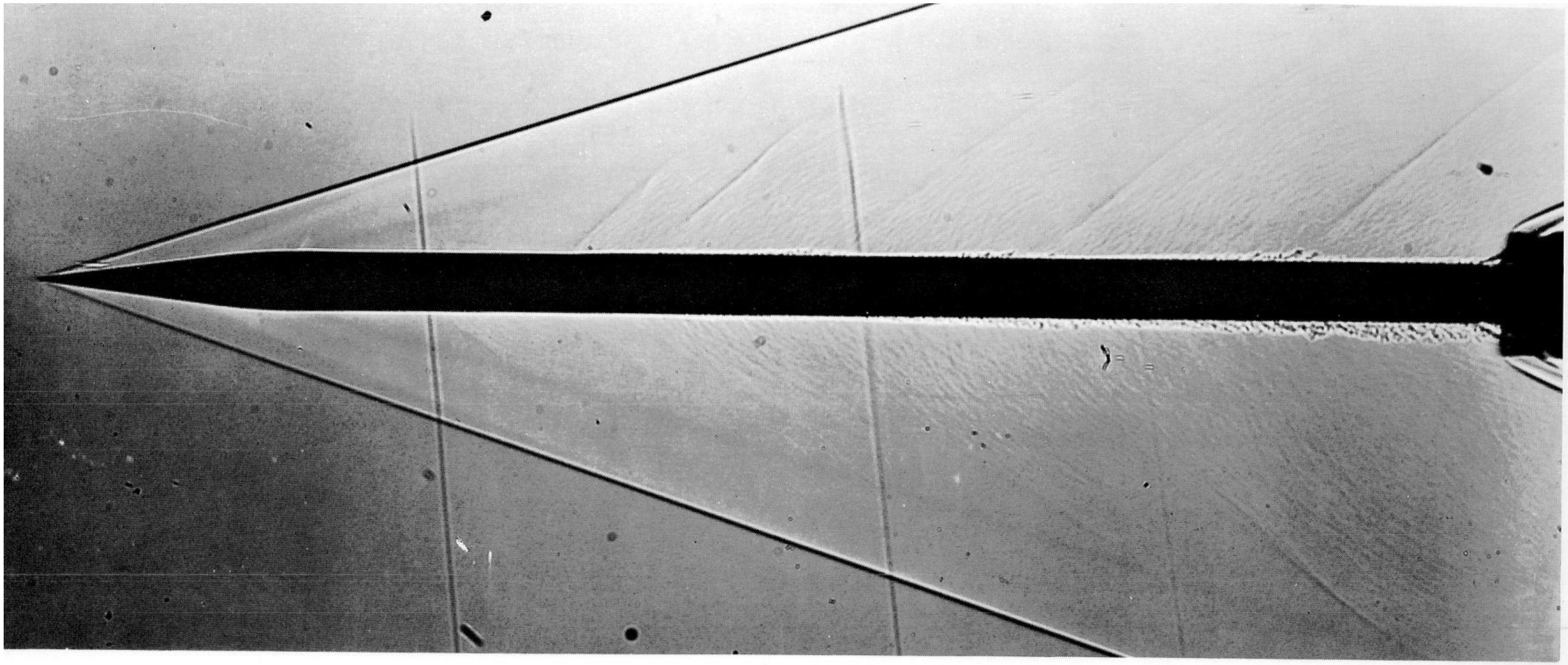

Shadowgraph of conical-nosed cylinder model in free flight; $M_\infty = 3.5$; $U_e/\nu = 2.1\times10^6$ per inch; H = 150 μin.; wind tunnel "air-off"; conical light field.

Transition to Turbulence

What are the dominant mechanisms of transition? Can we control it?

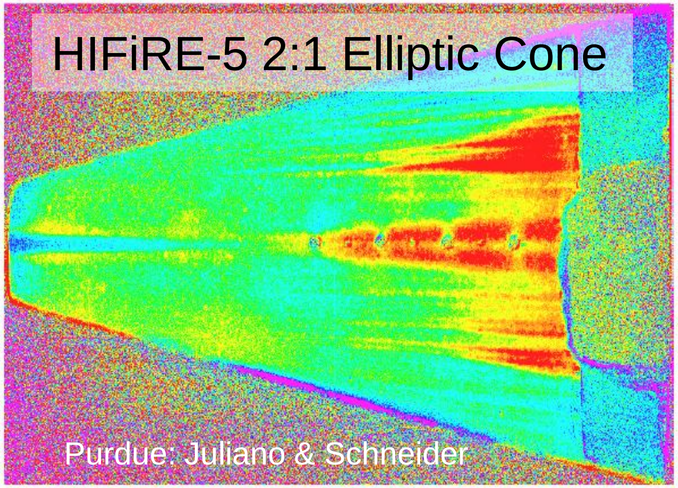

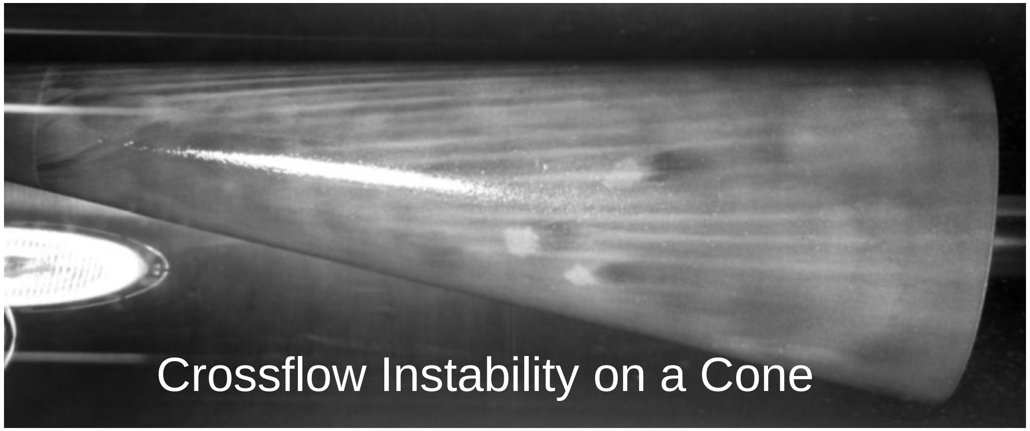

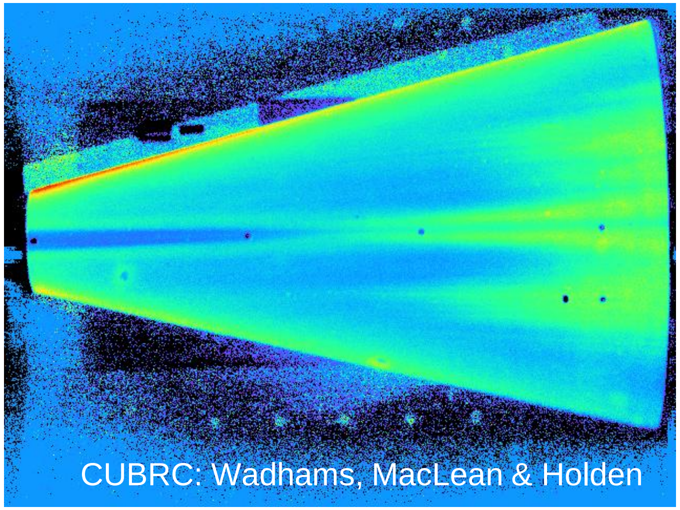

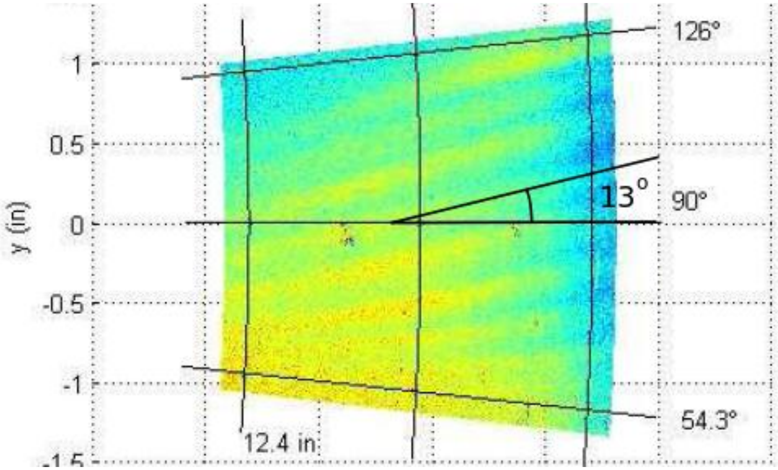

Swanson and Schneider

Turbulent Heat Flux

Why are turbulence model inaccurate? How can we fix them?

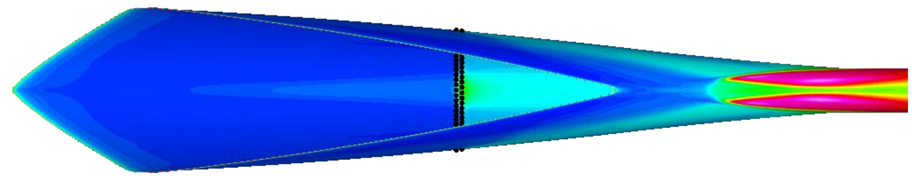

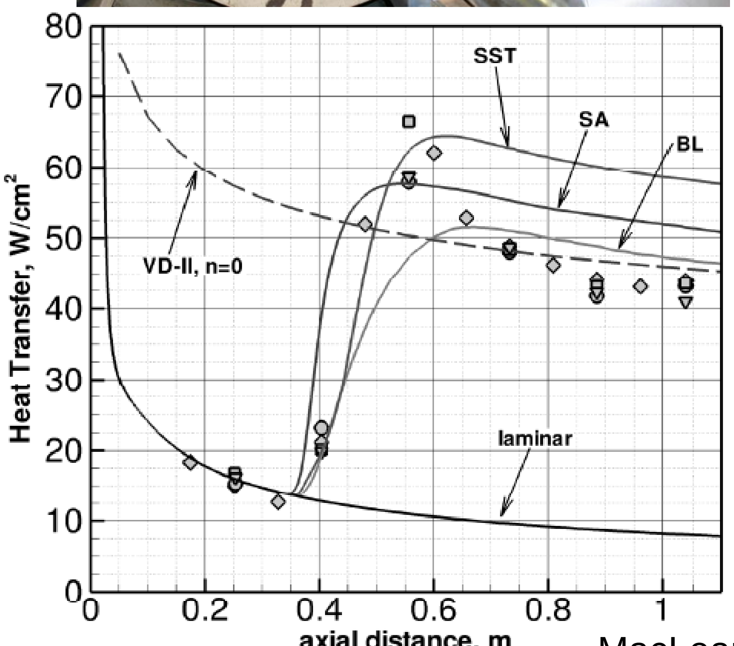

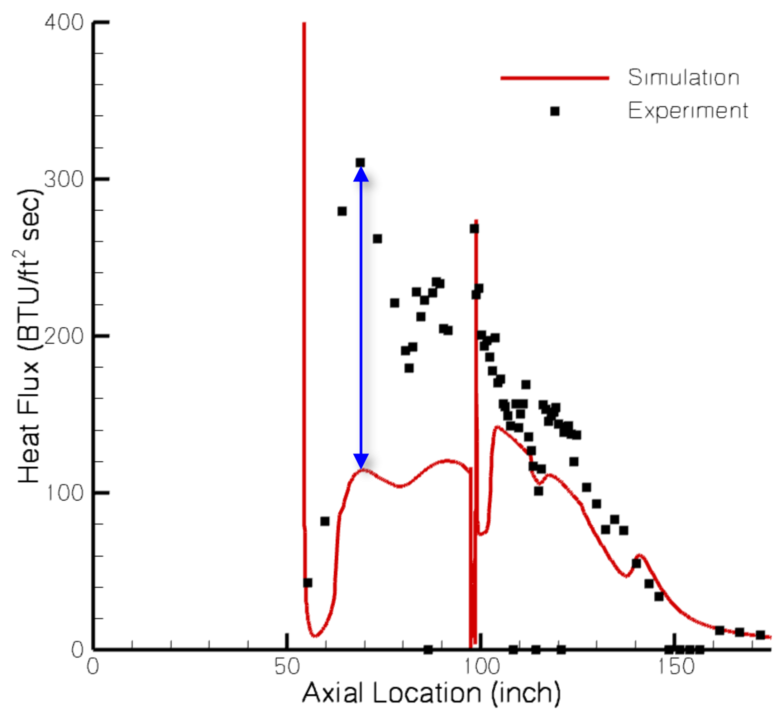

MacLean et al. 2009

Scramjet Fuel Injection

Can we resolve the dominant unsteadiness? At reasonable cost?

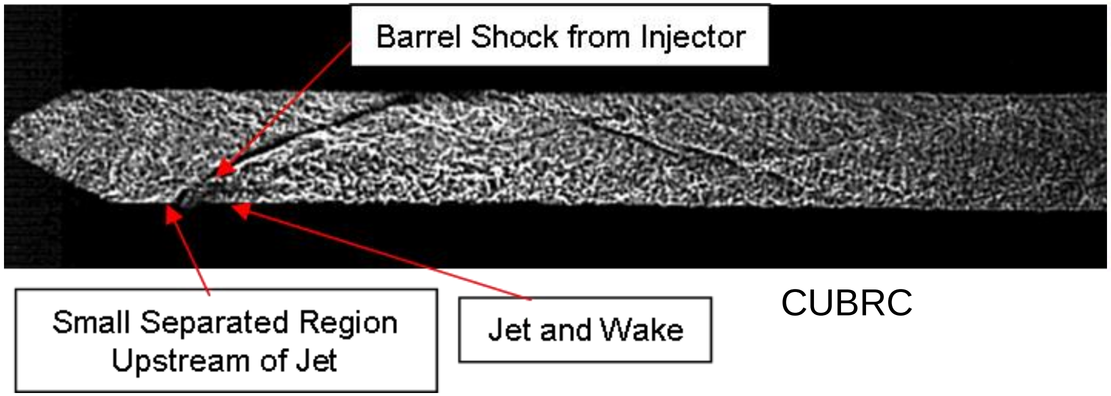

CUBRC

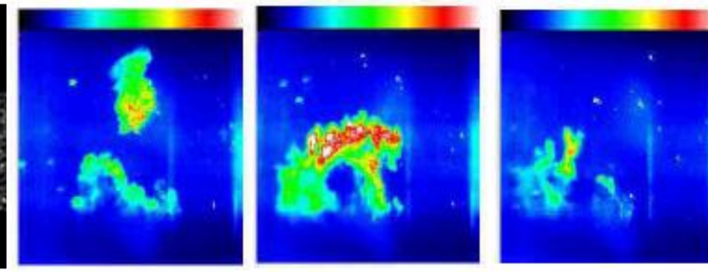

Instantaneous Fuel Concentration
Buggele and Seasholtz (1997)

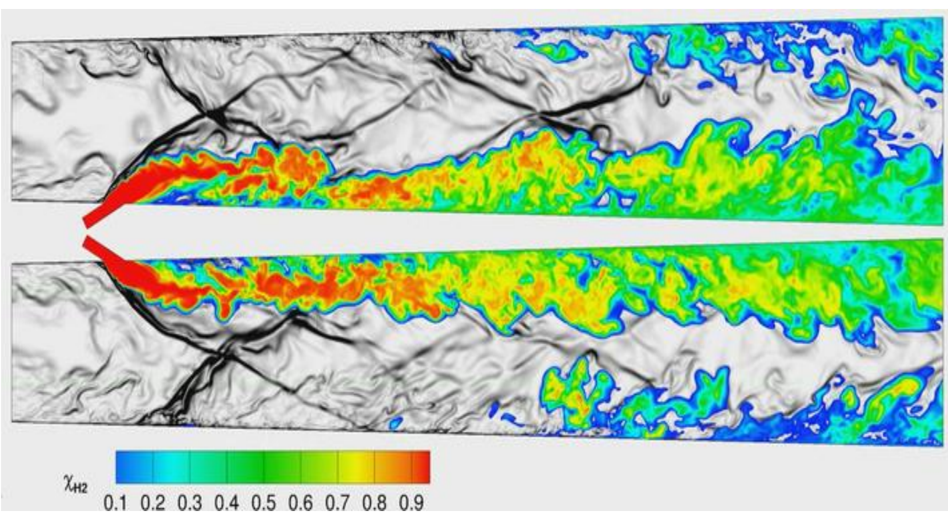

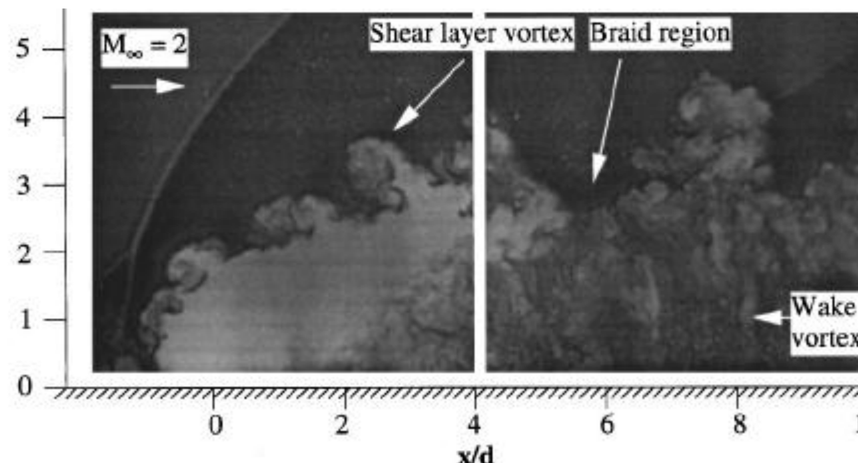

Gruber et al (1997)

STS-119: Comparison with HYTHIRM Data

HYTHIRM Data

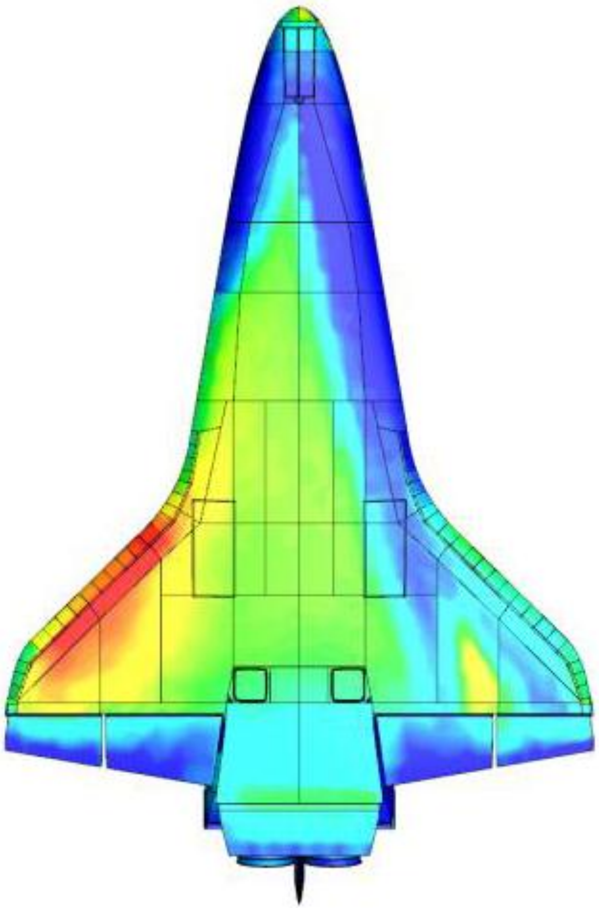

Horvath et al.

RANS Simulation

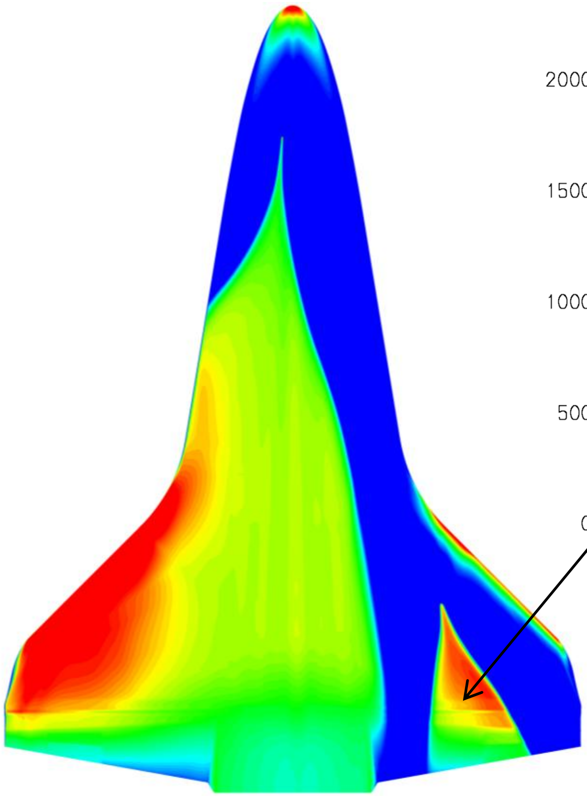

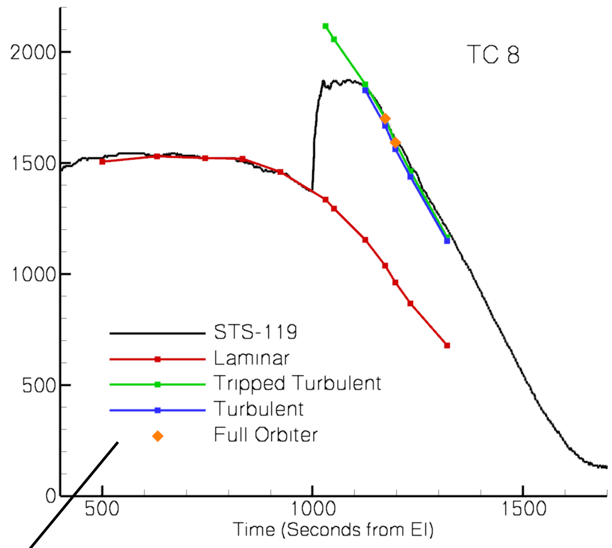

40 M elements

5-species finite-rate air

Radiative equilibrium (ε = 0.89)

A trivial calculation on 500 cores, but BL trip location is specified:

Not a prediction.

Inviscid Mach 12 Cylinder Flow

49k Hexahedral Elements

575k Tetrahedral Elements

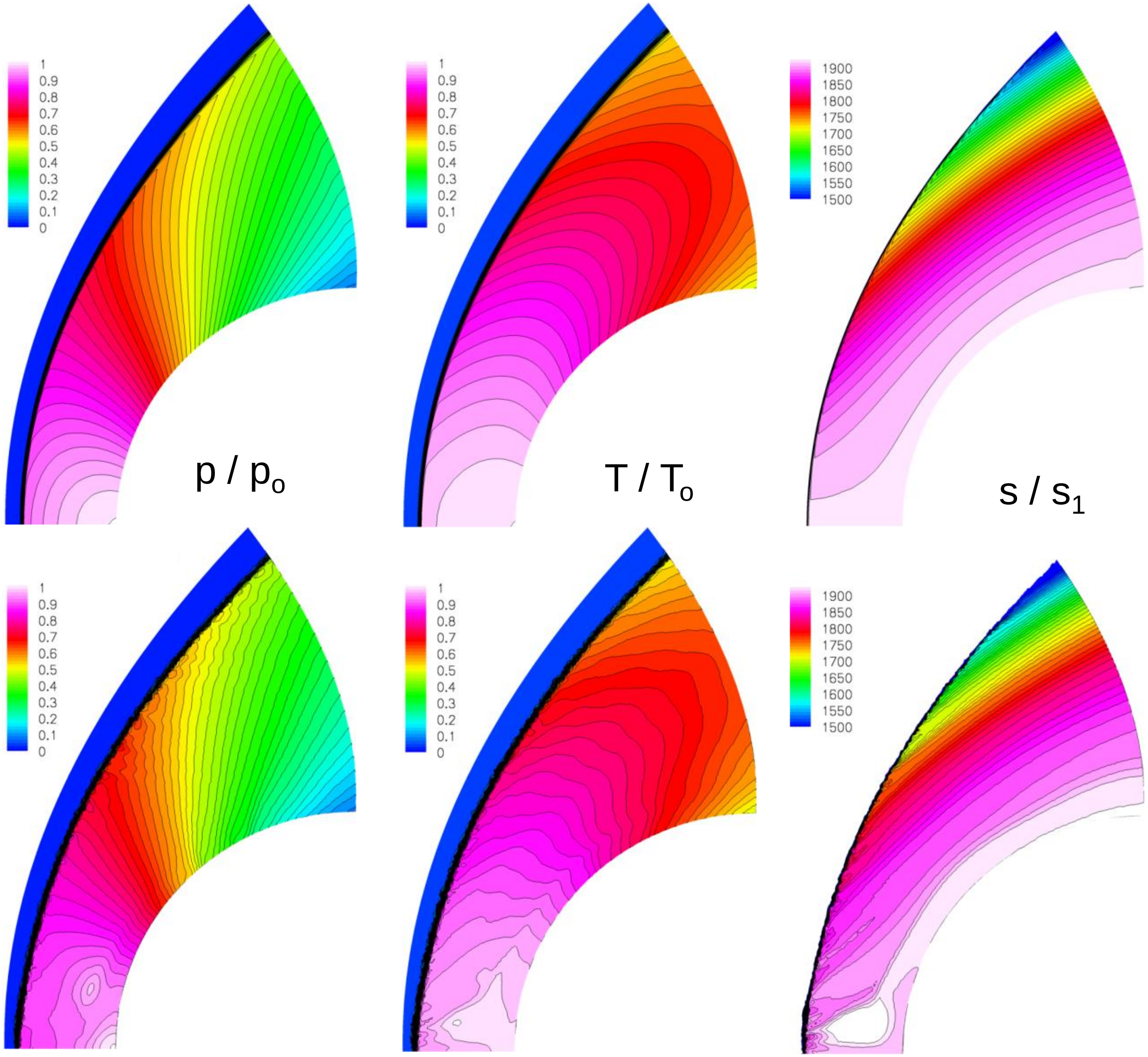

Future Directions in CFD for High-Speed Flows

- More complicated flow and thermo-chemical models:
  - Much larger numbers of chemical species / states
  - Detailed internal energy models
  - More accurate representation of ablation
  - Hybrid continuum / DSMC / molecular dynamics
  - Improved RANS models

- Unsteady flows:
  - Instability growth, transition to turbulence
  - Shape-change due to ablation
  - Fluid-structure interactions
  - Control systems and actuators in the loop
  - Wall-modeled LES on practical problems

Implicit Methods

- Cost scaling of current methods:
  - Quadratic with # of species
  - Implicit solve dominates
  - Memory intensive
- Need more species/equations:
  - C ablation = 16 species
  - HCN ablation = 38 species
  - Combustion
  - Internal energies
  - Turbulence closure

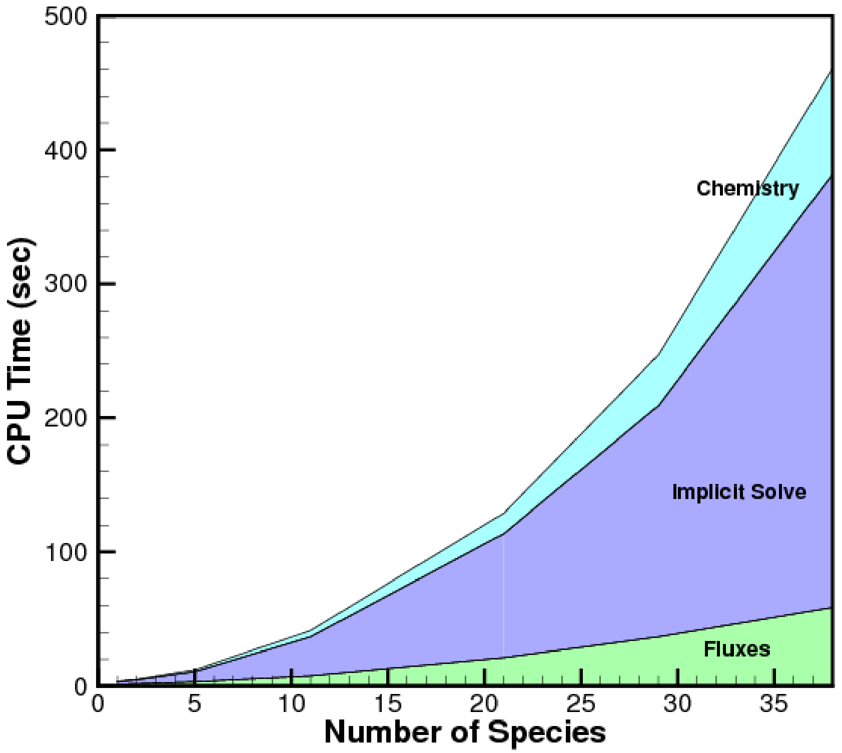

Computational cost of the DPLR Method

Background: DPLR Method

Discrete Navier-Stokes equations:

$$\frac{\partial U^n}{\partial t} + \frac{1}{V}\sum_f \left(F'^{n+1}S\right)^f = W^{n+1}$$

$$U = \begin{pmatrix} \rho_1 \\ \vdots \\ \rho_{ns} \\ \rho u \\ \rho v \\ \rho w \\ E_v \\ E \end{pmatrix}, \qquad F' = \begin{pmatrix} \rho_1 u' \\ \vdots \\ \rho_{ns} u' \\ \rho u u' + p s_x \\ \rho v u' + p s_y \\ \rho w u' + p s_z \\ E_v u' \\ (E+p)u' \end{pmatrix}$$

Linearize in time:

$$F'^{n+1} \simeq F'^n + \frac{\partial F'}{\partial U}^n \delta U^n$$

$$W^{n+1} \simeq W^n + \frac{\partial W}{\partial U}^n \delta U^n$$

Solve on grid lines away from wall using relaxation:

$\delta U^{(0)} = 0$

`for` $k = 1, k_{\max}$

$$\frac{\delta U^{(k)}}{\Delta t} + \frac{1}{V}\sum_{f=\ell}\left(A^{+f}\delta U^L + A^{-f}\delta U^R\right)^{(k)} S^f - \frac{\partial W}{\partial U}^n \delta U^{(k)} = -\frac{1}{V}\sum_f \left(F'^n S\right)^f + W^n$$
$$- \frac{1}{V}\sum_{f\neq\ell}\left(A^{+f}\delta U^L + A^{-f}\delta U^R\right)^{(k-1)} S^f$$

`end`

$$\delta U^n = \delta U^{(k_{\max})}$$

Background: DPLR Method

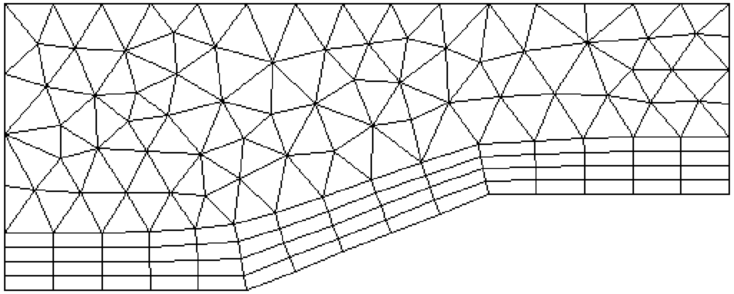

Discrete Navier-Stokes equations:

$$\frac{\partial U^n}{\partial t} + \frac{1}{V}\sum_f \left(F'^{n+1}S\right)^f = W^{n+1}$$

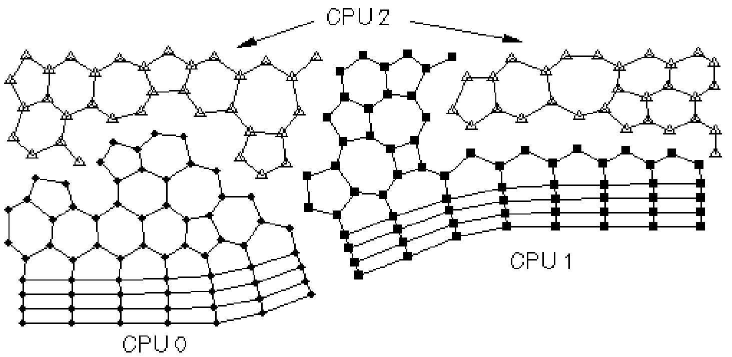

Linearize in time:

$$F'^{n+1} \simeq F'^n + \frac{\partial F'}{\partial U}^n \delta U^n$$

$$W^{n+1} \simeq W^n + \frac{\partial W}{\partial U}^n \delta U^n$$

Solve on grid lines away from wall using relaxation:

$$\delta U^{(0)} = 0$$

$\texttt{for}\ k = 1, k_{\max}$

$$\frac{\delta U^{(k)}}{\Delta t} + \frac{1}{V}\sum_{f=\ell}\left(A^{+f}\delta U^L + A^{-f}\delta U^R\right)^{(k)} S^f - \frac{\partial W}{\partial U}^n \delta U^{(k)} = -\frac{1}{V}\sum_f \left(F'^n S\right)^f + W^n - \frac{1}{V}\sum_{f\neq\ell}\left(A^{+f}\delta U^L + A^{-f}\delta U^R\right)^{(k-1)} S^f$$

$\texttt{end}$

$$\delta U^n = \delta U^{(k_{\max})}$$

Background: DPLR Method

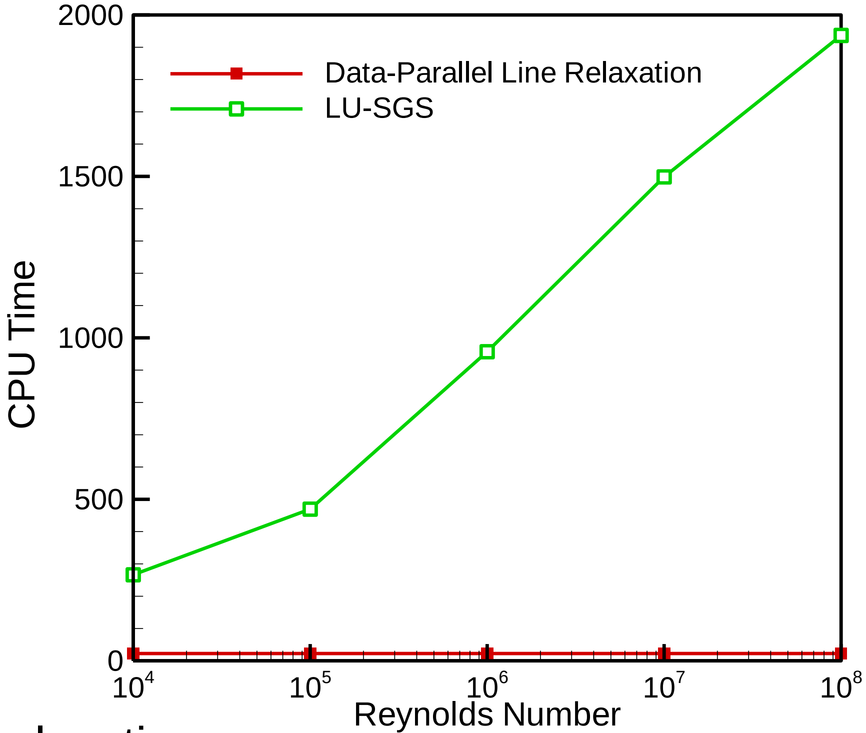

Discrete Navier-Stokes equations:

$$\frac{\partial U^n}{\partial t} + \frac{1}{V}\sum_f \left(F'^{n+1} S\right)^f = W^{n+1}$$

Linearize in time:

$$F'^{n+1} \simeq F'^n + \frac{\partial F'}{\partial U}^n \delta U^n$$

$$W^{n+1} \simeq W^n + \frac{\partial W}{\partial U}^n \delta U^n$$

Solve on grid lines away from wall using relaxation:

$\delta U^{(0)} = 0$

$\texttt{for}\ k = 1, k_{\max}$

$$\frac{\delta U^{(k)}}{\Delta t} + \frac{1}{V}\sum_{f=\ell}\left(A^{+f}\delta U^L + A^{-f}\delta U^R\right)^{(k)} S^f - \frac{\partial W}{\partial U}^n \delta U^{(k)} = -\frac{1}{V}\sum_f \left(F'^n S\right)^f + W^n - \frac{1}{V}\sum_{f\neq\ell}\left(A^{+f}\delta U^L + A^{-f}\delta U^R\right)^{(k-1)} S^f$$

$\texttt{end}$

$$\delta U^n = \delta U^{(k_{\max})}$$

Decoupled Implicit Method

Split equations:

$$\frac{\partial \tilde{U}}{\partial t} + \frac{1}{V}\sum_f \left(\tilde{F}'^{n+1} S\right)^f = 0$$

$$\frac{\partial \hat{U}}{\partial t} + \frac{1}{V}\sum_f \left(\hat{F}'^{n+1} S\right)^f = \hat{W}^{n+1}$$

$$\tilde{U} = \rho \begin{pmatrix} \rho \\ \rho u \\ \rho v \\ \rho w \\ E \end{pmatrix}, \quad \hat{U} = \rho \begin{pmatrix} c_1 \\ \vdots \\ c_{ns} \\ e_v \end{pmatrix} = \rho \hat{V}$$

Solve in two steps:

First use DPLR for $\tilde{U}$, then a modified form of DPLR for $\hat{V}$

$$\hat{W}^{n+1} = \hat{W}(\tilde{U}^{n+1}, \hat{V}^{n+1}) \simeq \hat{W}(\tilde{U}^{n+1}, \hat{V}^{n}) + \left.\frac{\partial \hat{W}}{\partial U}\right|_{\tilde{U}} \frac{\partial U}{\partial \hat{V}} \delta \hat{V}^n$$

$$C = \left.\frac{\partial \hat{W}}{\partial U}\right|_{\tilde{U}} \frac{\partial U}{\partial \hat{V}} \qquad \chi = \mathrm{diag}(C)$$

$$C\delta\hat{V} = \chi\delta\hat{V} + (C - \chi)\delta\hat{V}$$ Lag the off-diagonal terms in source term Jacobian

Comparison of Implicit Problems

DPLR **block** tridiagonal solve (2D):

$$\begin{pmatrix} \ddots & \ddots & \ddots & & & \\ & \square & \square & \square & & \\ & & \square & \square & \square & \\ & & & \square & \square & \square \\ & & & \ddots & \ddots & \ddots \end{pmatrix} \begin{pmatrix} \vdots \\ \delta U_{i,j-1} \\ \delta U_{i,j} \\ \delta U_{i,j+1} \\ \vdots \end{pmatrix}^{(k)} = \begin{pmatrix} \vdots \\ \mathrm{RHS}_{i,j} \\ \vdots \end{pmatrix}^{n} - \square\, \delta U^{(k-1)}_{i+1,j} - \square\, \delta U^{(k-1)}_{i-1,j}$$

ne x *ne* block matrices

Decoupled **scalar** tridiagonal solve:

$$\begin{pmatrix} \ddots & \ddots & \ddots & & & \\ & \diagdown & \diagdown & \diagdown & & \\ & & \diagdown & \diagdown & \diagdown & \\ & & & \diagdown & \diagdown & \diagdown \\ & & & \ddots & \ddots & \ddots \end{pmatrix} \begin{pmatrix} \vdots \\ \delta \hat{V}_{i,j-1} \\ \delta \hat{V}_{i,j} \\ \delta \hat{V}_{i,j+1} \\ \vdots \end{pmatrix}^{(k)} = \begin{pmatrix} \vdots \\ \mathrm{R\hat{H}S}_{i,j} \\ \vdots \end{pmatrix}^{n} - \diagdown\, \delta \hat{V}^{(k-1)}_{i+1,j} - \diagdown\, \delta \hat{V}^{(k-1)}_{i-1,j} + \boxbslash\, \delta \hat{V}^{(k-1)}_{i,j}$$

quadratic term

Does it Work?

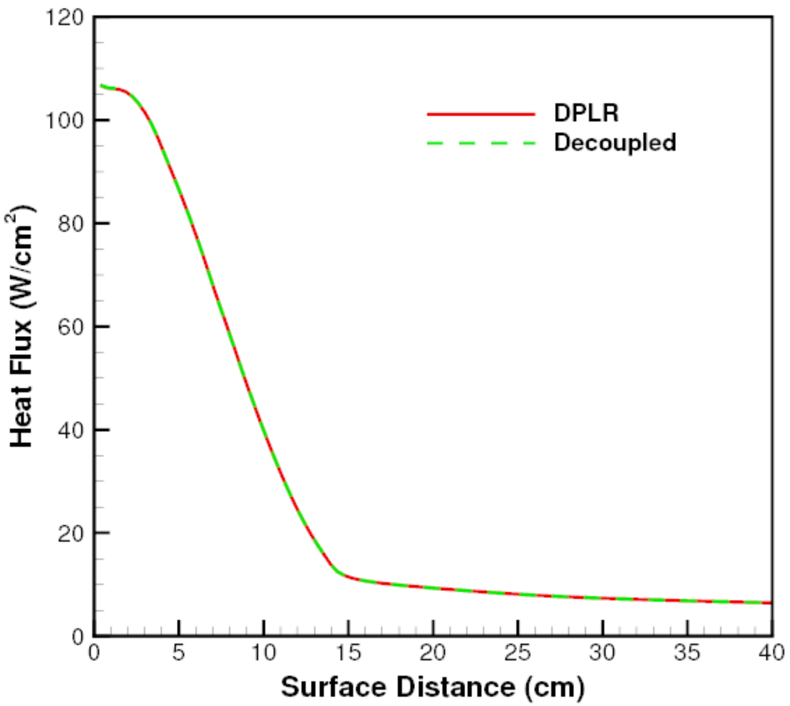

Surface heat flux for 21-species Air-CO_2 mixture at Mach 15

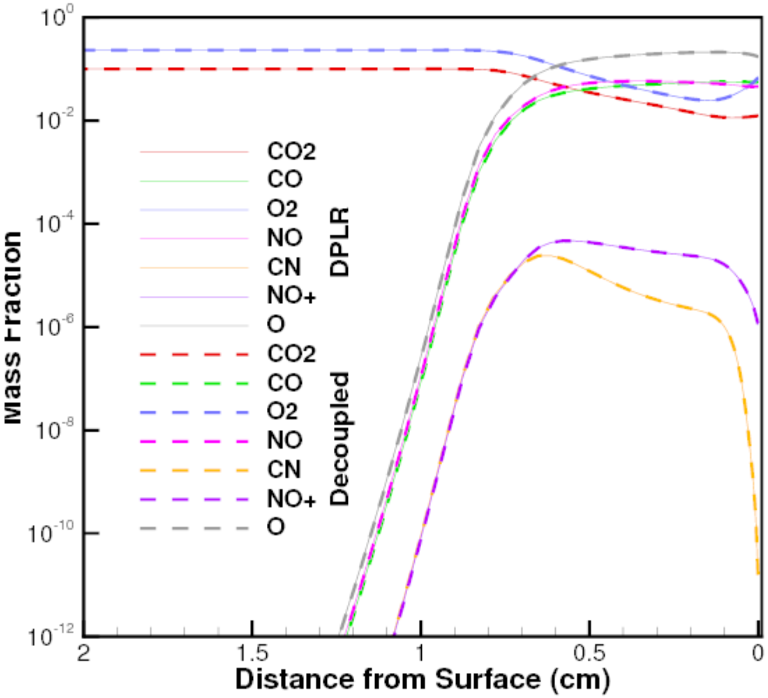

Chemical species on stagnation streamline

But, must have: $$\sum_s F'_{\rho_s} = F'_{\rho}$$

Comparison of Convergence History

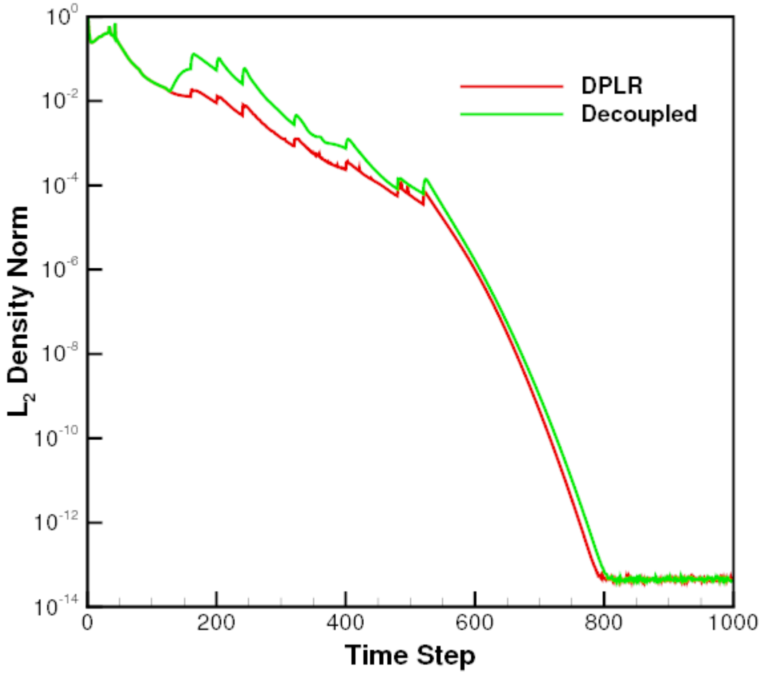

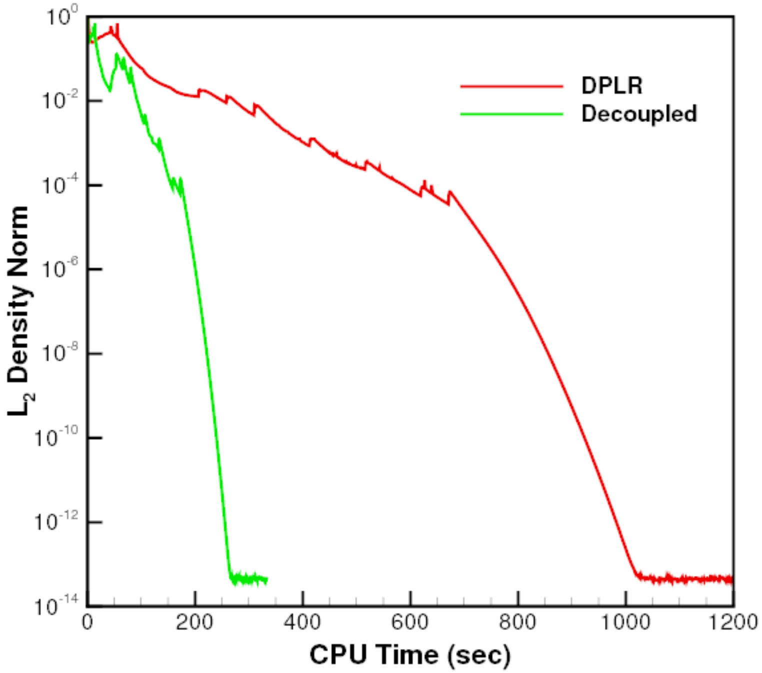

Mach 15, 21-species, 32-reaction air-CO_2 kinetics model on a resolved grid
10 cm radius sphere – 8º cone; results are similar at different M, Re, etc.

Extensive comparisons for double-cone flow at high enthalpy conditions

Comparison of Computational Cost

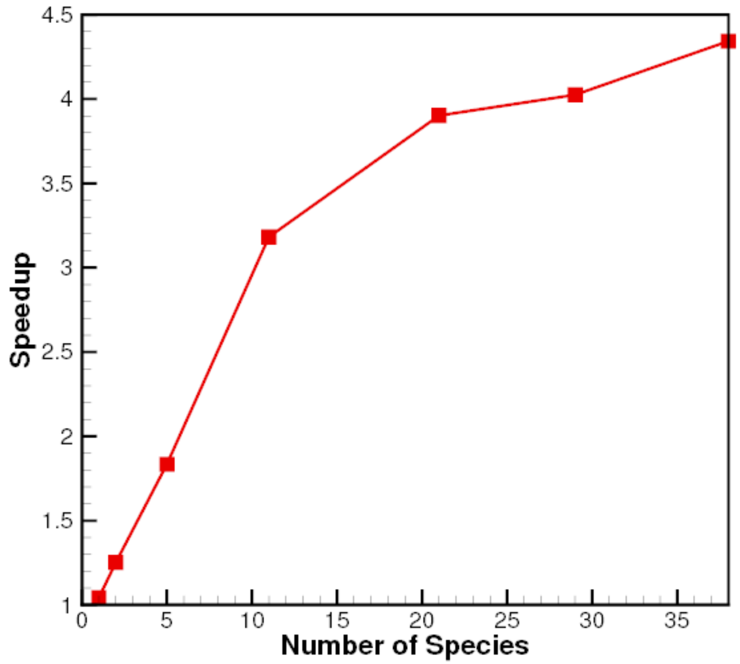

Computer Time Speedup

Memory reduction ~ 7X

Source term now dominates cost

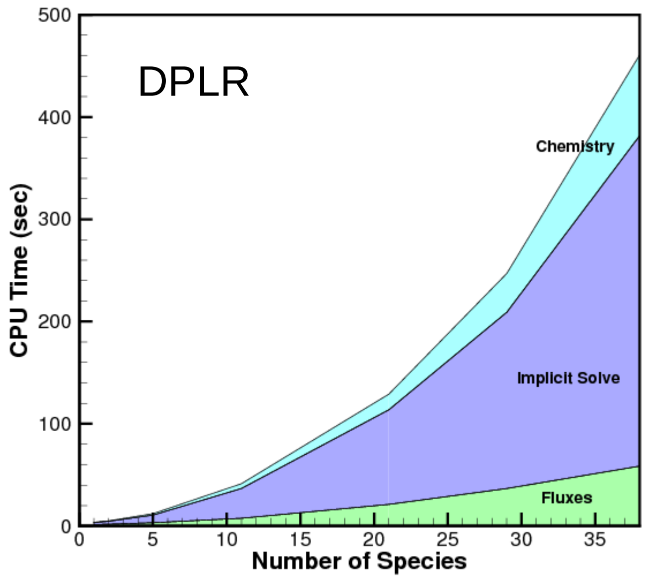

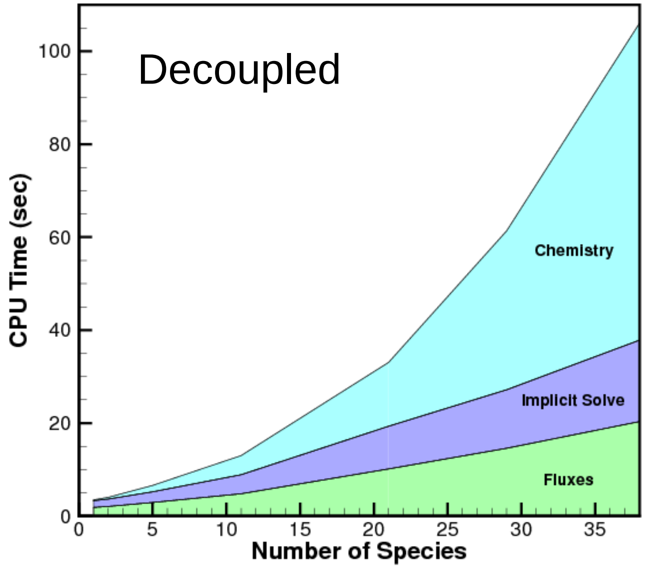

Low-Dissipation Numerical Methods

- Most CFD methods for high-speed flows use upwind methods:
  - Designed to be dissipative
  - Good for steady flows
  - Dissipation can overwhelm the flow physics

- Develop a new numerical flux function:
  - Discrete kinetic energy flux consistent with the KE equation
  - Add upwind dissipation using shock sensor
  - 2nd, 4th and 6th order accurate formulations

- Other similar approaches are available

Kinetic Energy Consistent Flux

- Usually solve for mass, momentum and total energy
- KE portion of the energy equation is redundant:
  - Only need the mass and momentum equations for KE
- Can we find a flux that is consistent between equations?

$$-k\frac{\partial \rho u_j}{\partial x_j} + u_i\frac{\partial \rho u_i u_j}{\partial x_j} = \frac{\partial \rho k u_j}{\partial x_j}$$

Spatial derivatives

$$-k\frac{\partial \rho}{\partial t} + u_i\frac{\partial \rho u_i}{\partial t} = \frac{\partial \rho k}{\partial t}$$

Time derivatives

mass momentum energy

- Always true at the PDE level; but not discretely (space/time)

Kinetic Energy Consistent Flux

- Derive fluxes that ensure that these relations hold discretely:

$$F_{\mathrm{f}}'^{*} = \rho_{\mathrm{f}} u_{\mathrm{f}}' \begin{bmatrix} 1 \\ \bar{u} \\ \bar{v} \\ \bar{w} \\ \tilde{k} \end{bmatrix}$$

Semi-discrete form

$$F_{\mathrm{f}}'^{*} = \rho_{\mathrm{f}} u_{\mathrm{f}}' \begin{bmatrix} 1 \\ \overline{u^\star} \\ \overline{v^\star} \\ \overline{w^\star} \\ \widetilde{k^\star} \end{bmatrix}_{\mathrm{f}}$$

Fully discrete form

$$\left(u^\star = \frac{\sqrt{\rho^{n+1}}u^{n+1} + \sqrt{\rho^n}u^n}{\sqrt{\rho^{n+1}} + \sqrt{\rho^n}} \right) \text{etc.}$$

- In practice, this approach is very stable
- Add dissipation with shock sensor

Subbareddy & Candler (2009)

Low-Dissipation Numerical Method

Compressible Mixing Layer

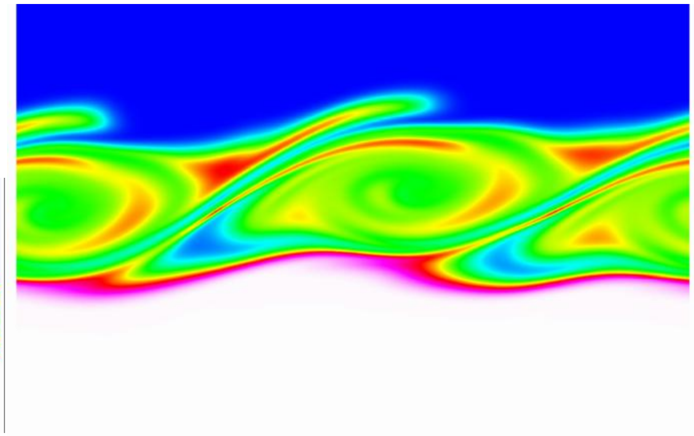

Conventional 3rd order upwind method

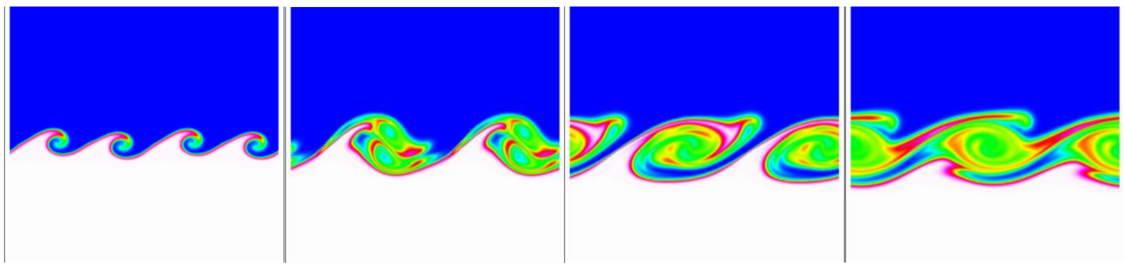

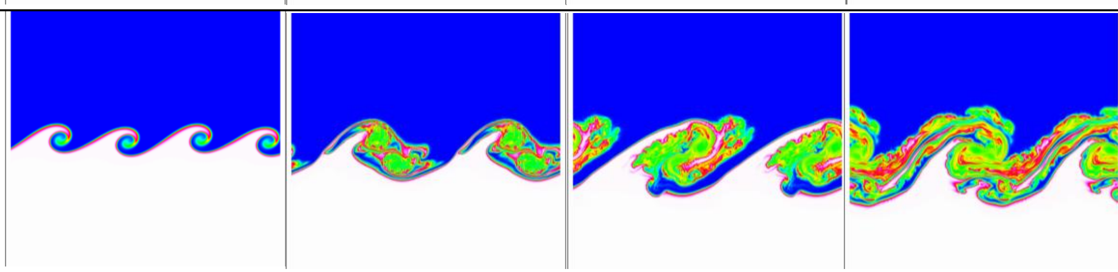

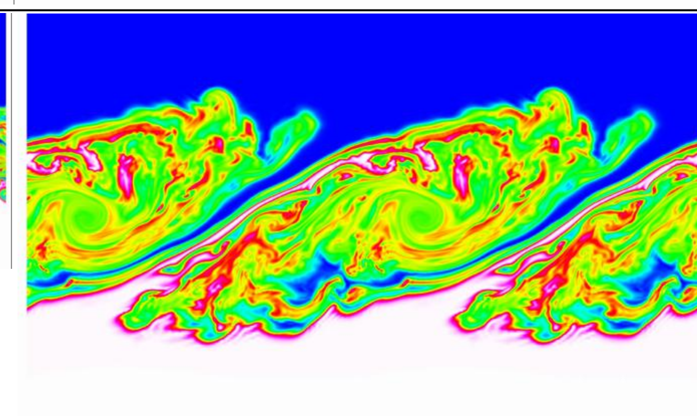

2nd order KE consistent method

Same cost, much more physics

Capsule Model on Sting

2nd order
KEC

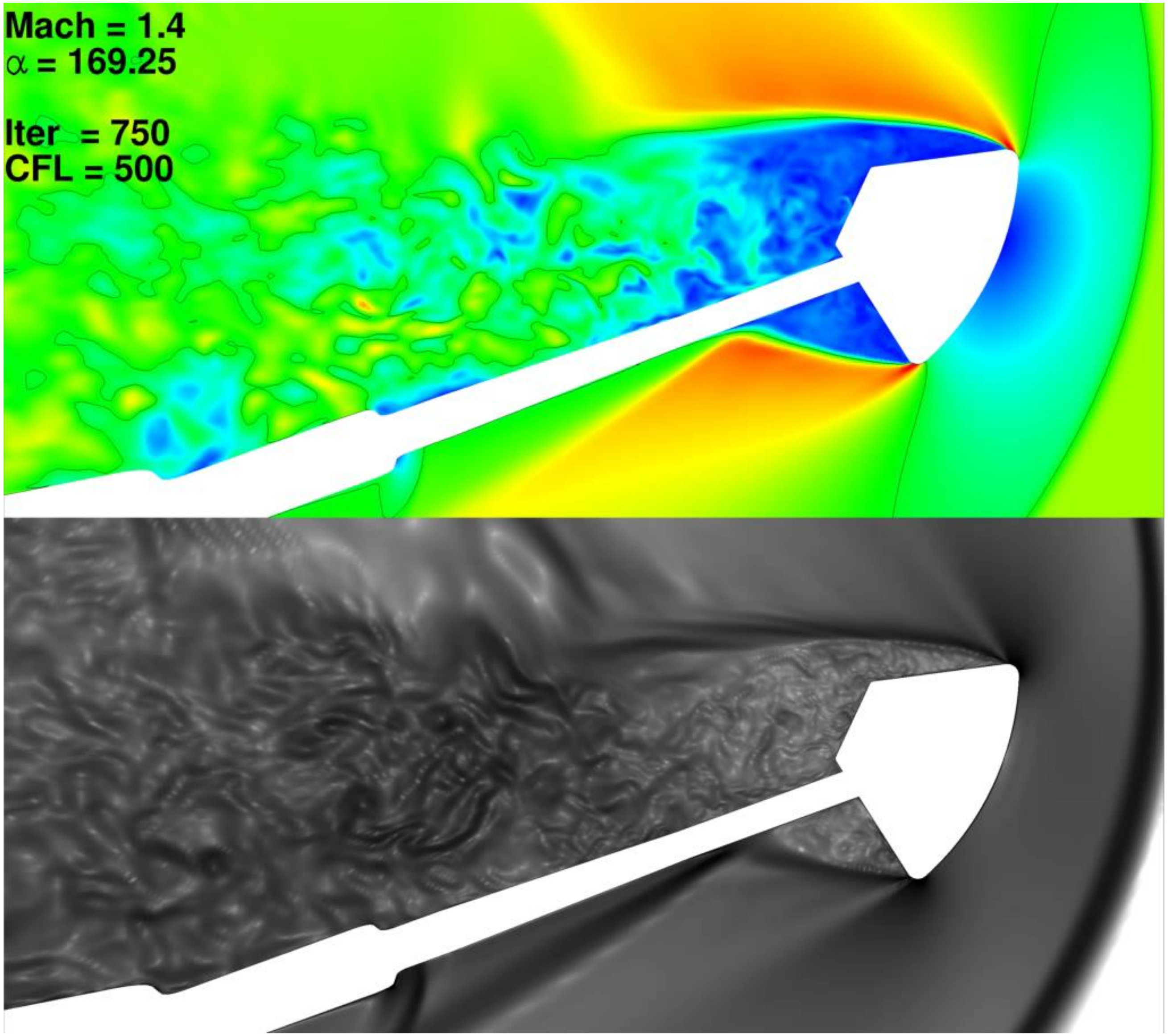

Schwing

Gradient Reconstruction for Higher Order

- For unstructured meshes, use a pragmatic approach:
  - Reconstruct the face variables using the cell-centered values and gradients
  - Requires minimal connectivity information

$$\phi_{\mathrm{f}}^{L} = \phi_i \quad + \alpha \left(\nabla\phi\right)_i \cdot \quad \left(\vec{x}_{\mathrm{f}} - \vec{x}_i\right)$$
$$\phi_{\mathrm{f}}^{R} = \phi_{i+1} + \alpha \left(\nabla\phi\right)_{i+1} \cdot \left(\vec{x}_{\mathrm{f}} - \vec{x}_{i+1}\right)$$
$$\phi_{\mathrm{f}} = \tfrac{1}{2}\left(\phi_{\mathrm{f}}^{L} + \phi_{\mathrm{f}}^{R}\right)$$

  - Pick α to give the exact 4th order derivative on a uniform grid
  - α controls the modified wavenumber and can be tuned
- Scheme is not exactly energy conserving Pirozzoli (2010)
- Higher-order only on smoothly-varying grids

Low-Dissipation Numerical Method

Propagation of a Gaussian density pulse

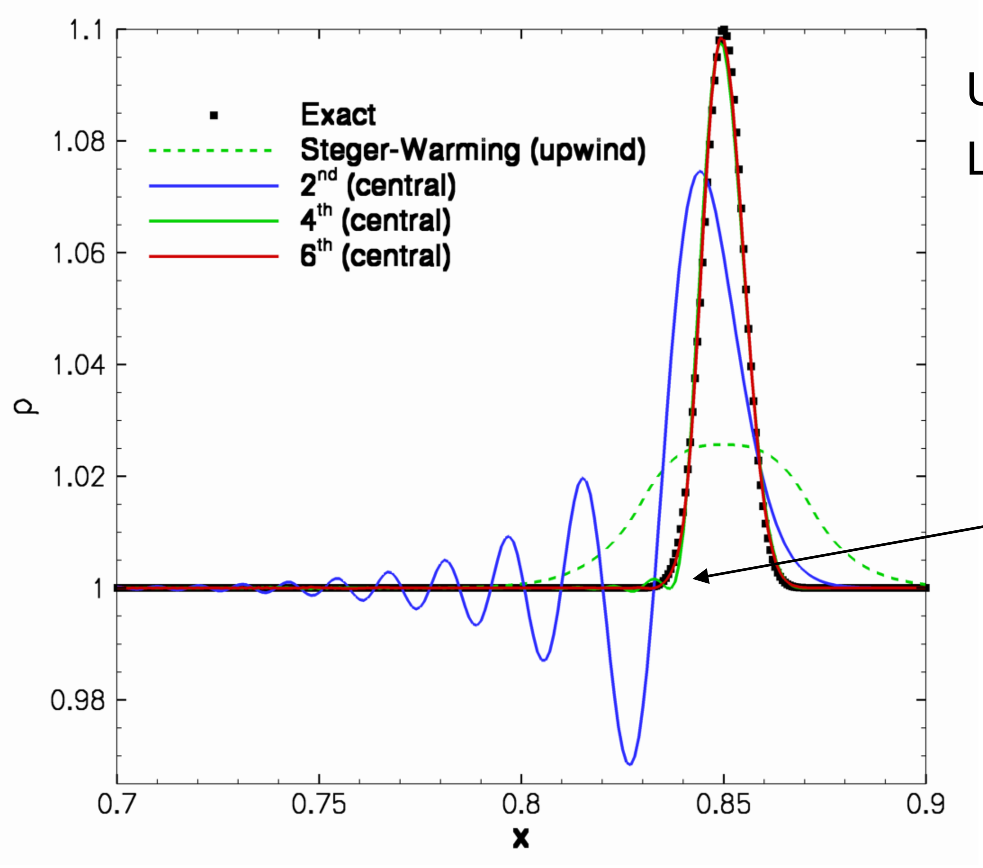

Subbareddy & Bartkowicz

Upwind methods rapidly damp solution

Low-order methods are dispersive

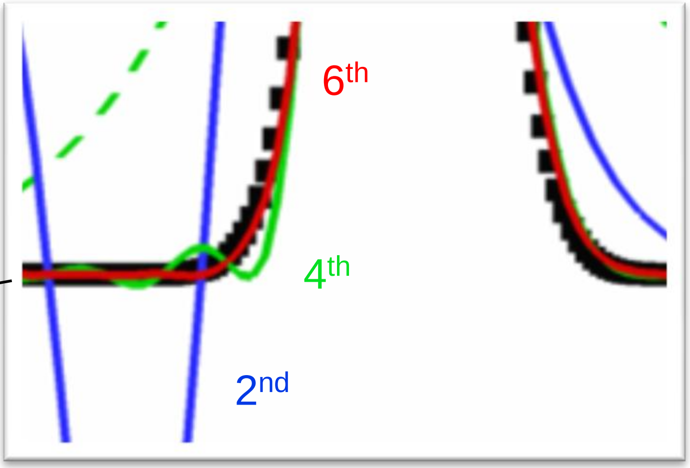

Enables a new class of simulations

Discrete Roughness Wake

Cylinder mounted in wall of Purdue Mach 6 Quiet Tunnel

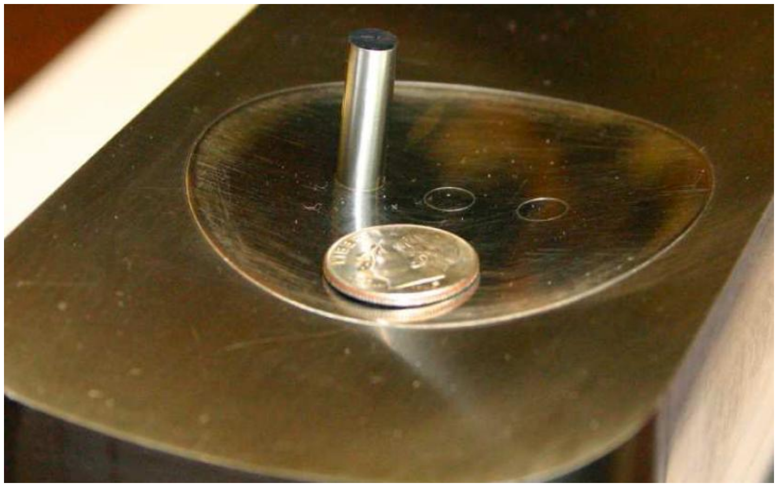

Wheaton & Schneider

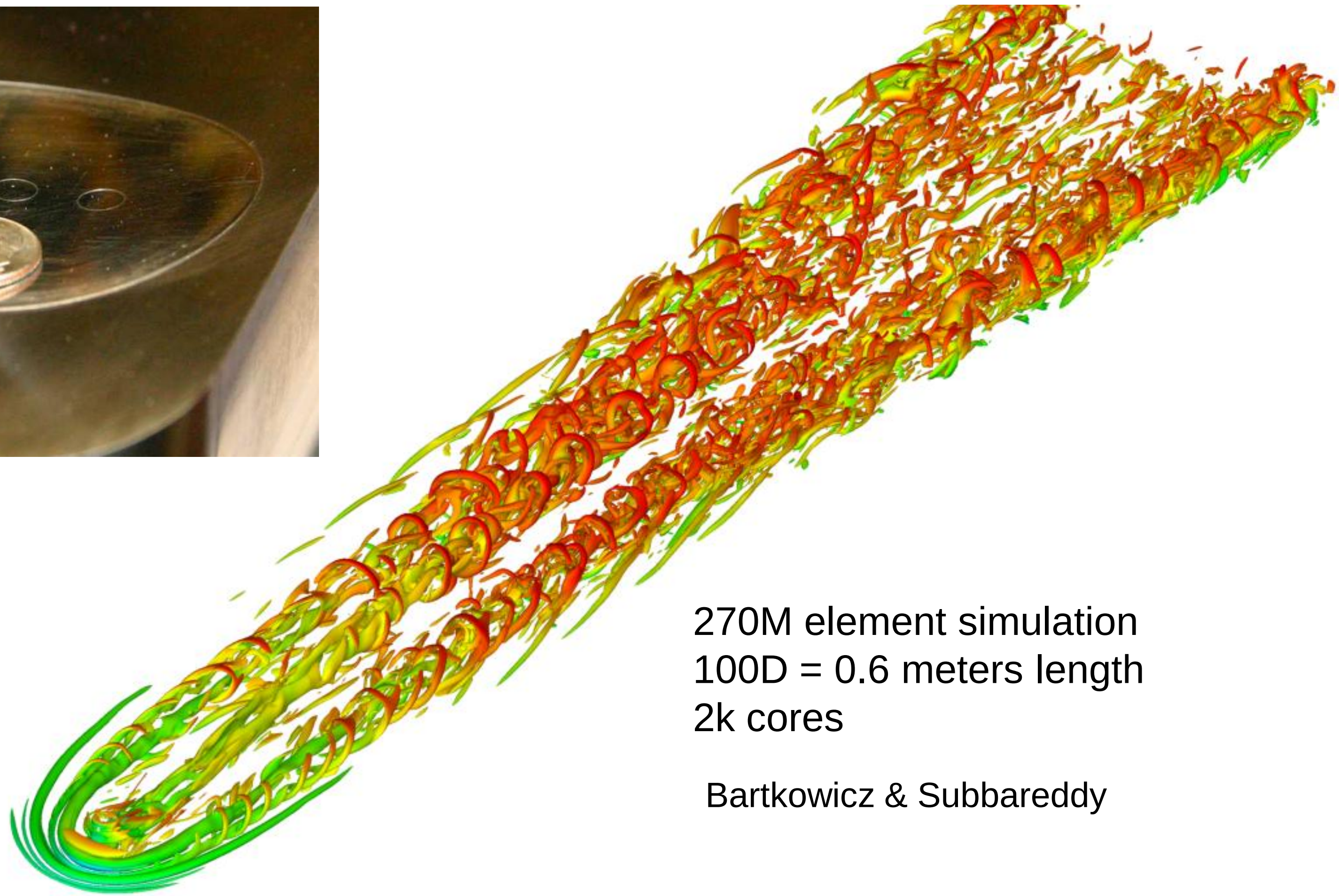

270M element simulation
100D = 0.6 meters length
2k cores

Bartkowicz & Subbareddy

Grid Generation

O(10) reduction in grid elements

Gridpro topology

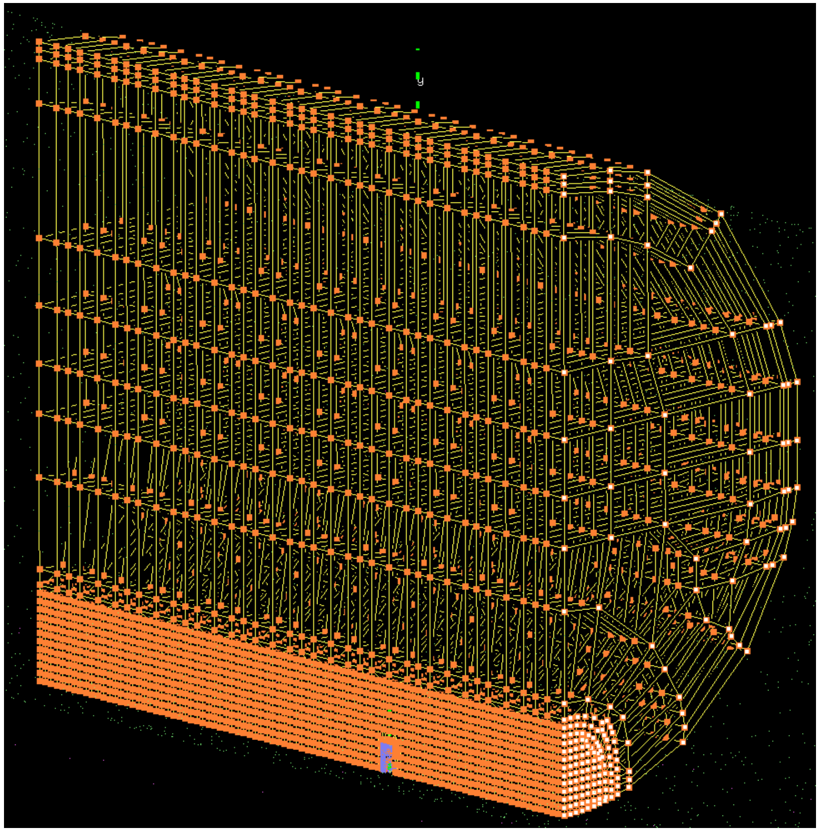

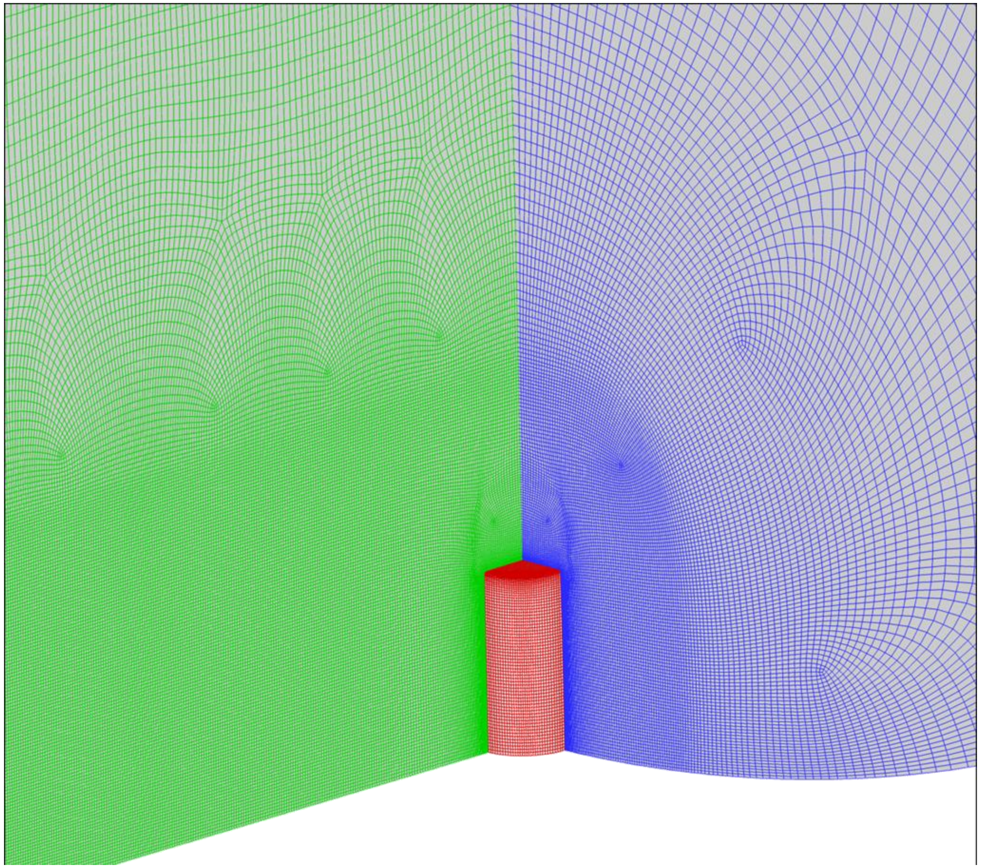

Grid near protuberance
(before wall clustering)

Discrete Roughness Wake

Comparison with experiment: Pressure fluctuations at x/D = -1.5

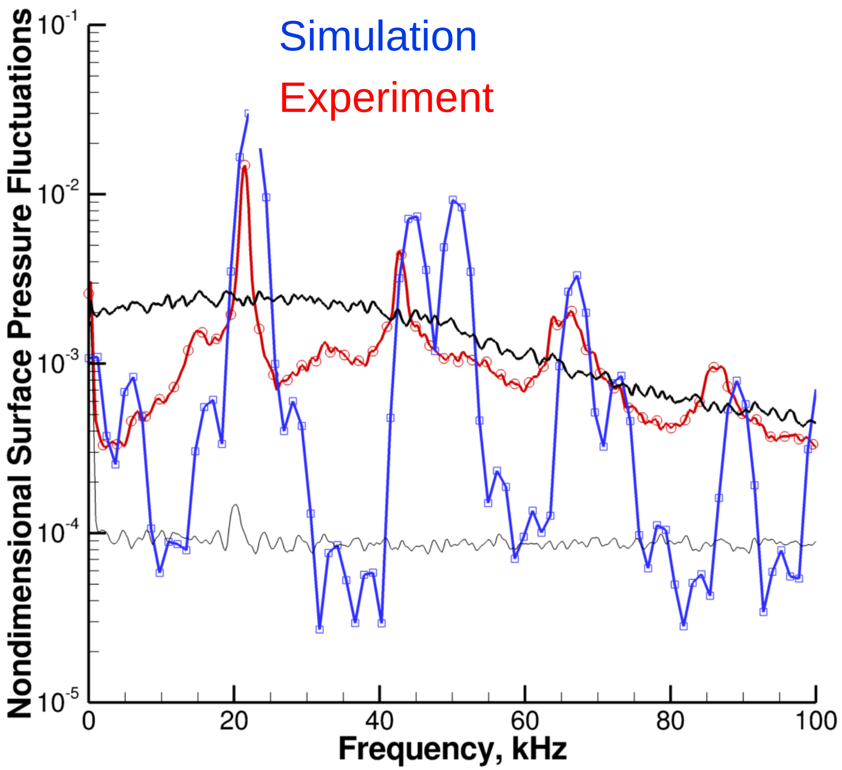

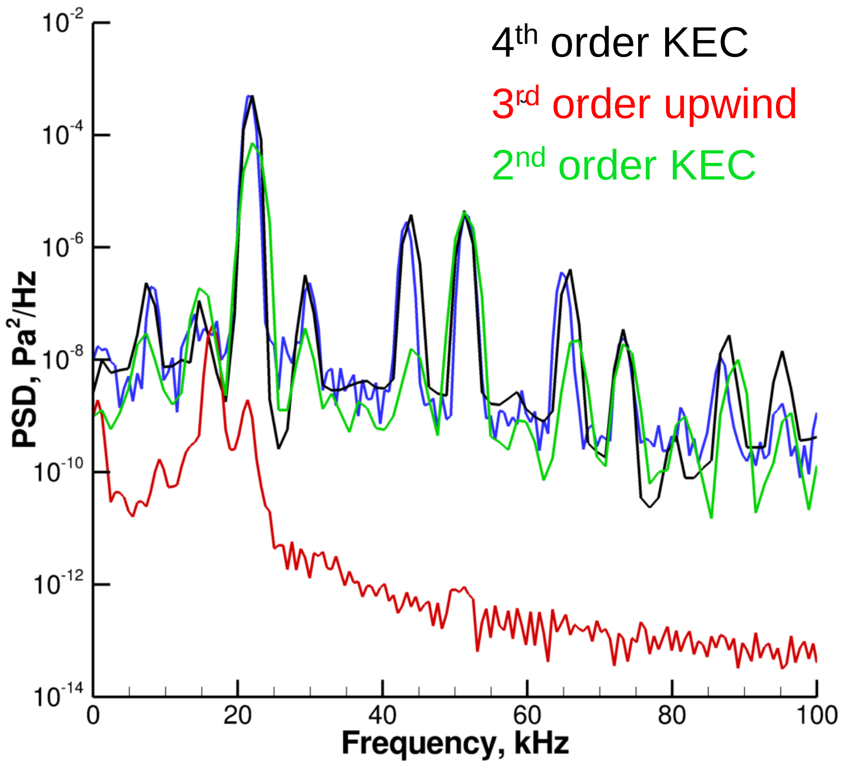

Impossible with upwind methods

Crossflow Instability on a Cone

Purdue M6 Quiet Tunnel experiments:

- 7^{o} cone, 41 cm long
- 0.002” (51 μm) nose radius

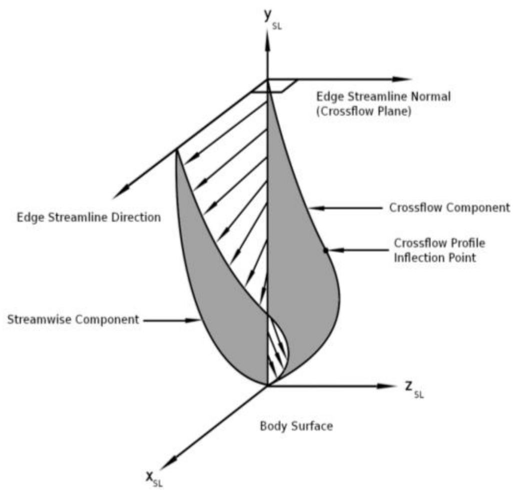

Random roughness on wind side:

- 10, 20 μm height (~ paint finish)

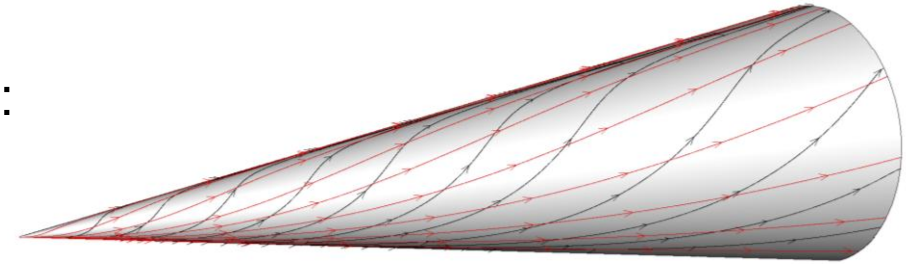

Surface and BL Edge Streamlines

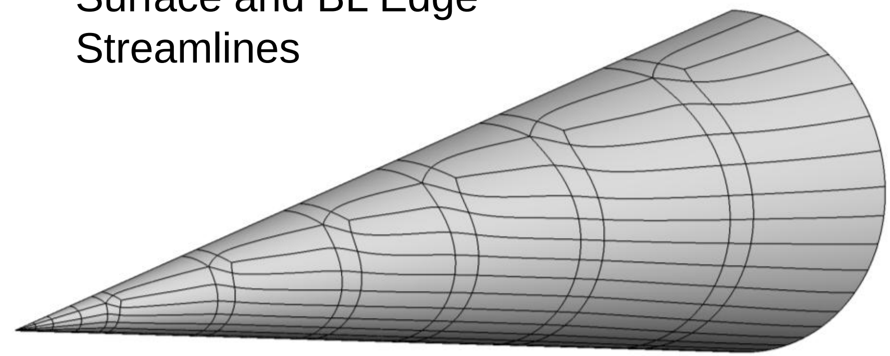

Grid Topology

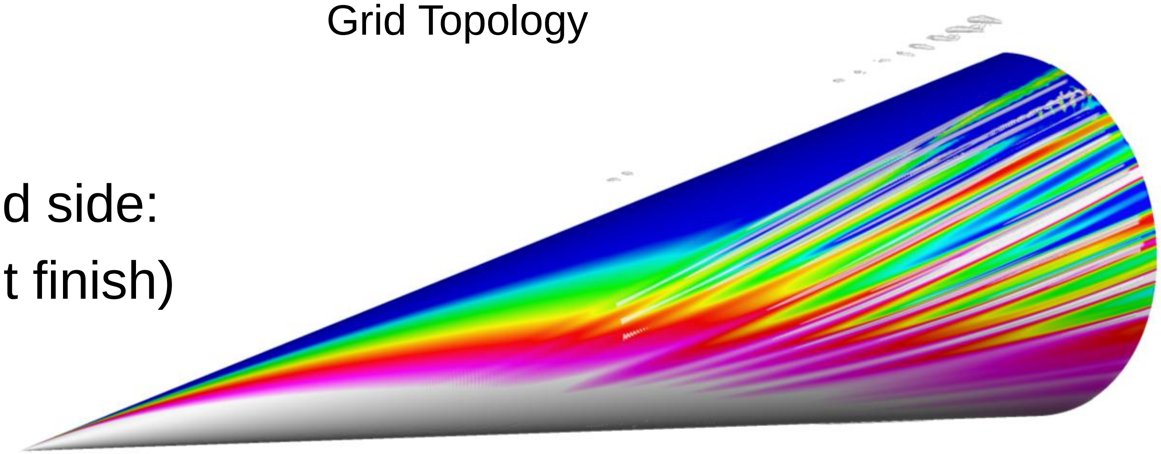

Gronvall AIAA-2012-2822

Crossflow Instability on a Cone

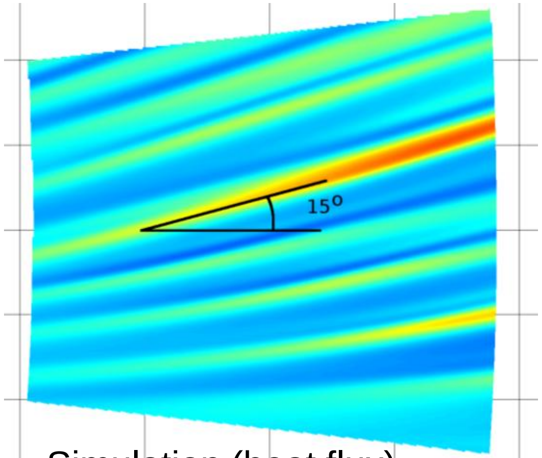

Simulation (heat flux)

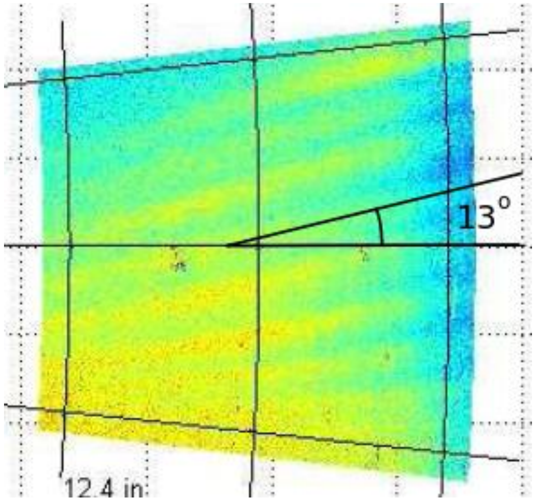

Purdue TSP Data (Swanson)

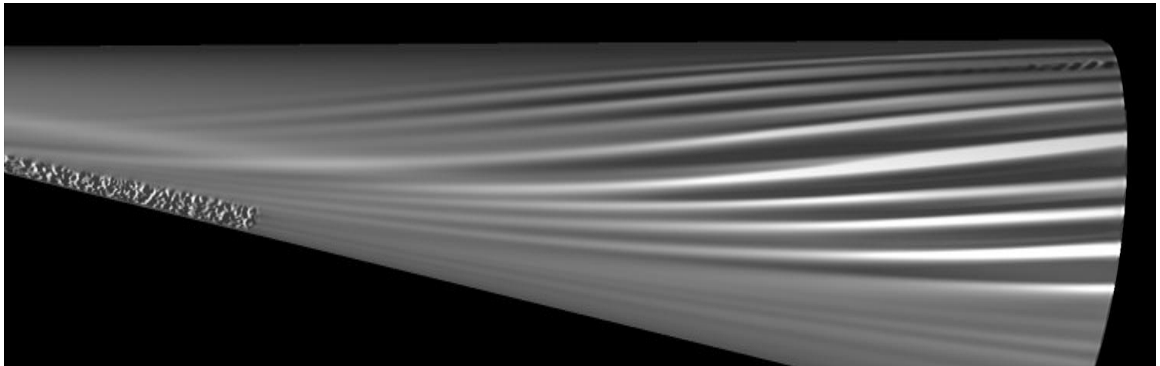

Simulation (shear stress)

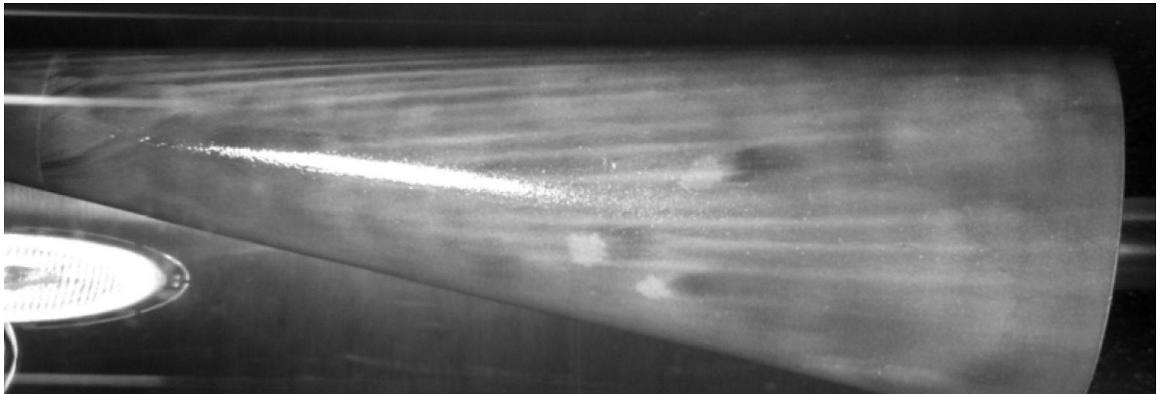

Purdue Oil Flow Experiment

Simulations of Capsule Dynamic Stability

6-DOF moving grid simulation

Capture wake unsteadiness

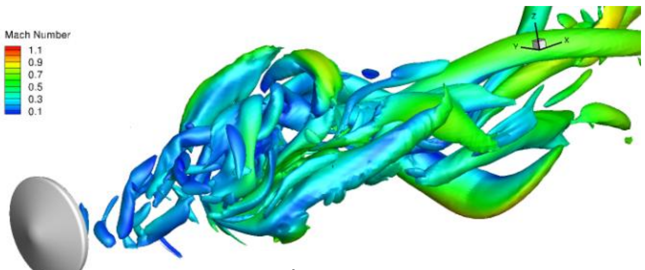

2nd Order Upwind

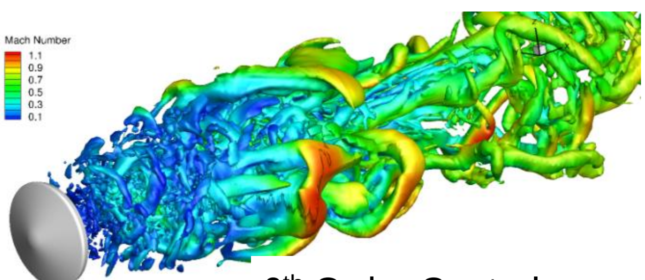

6th Order Central

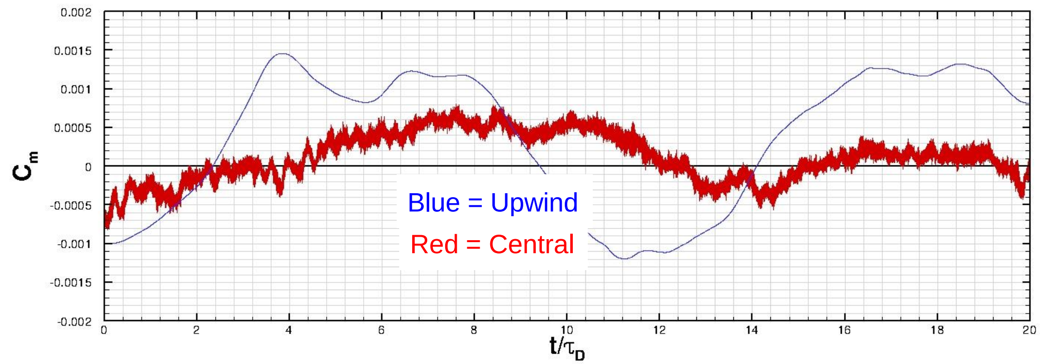

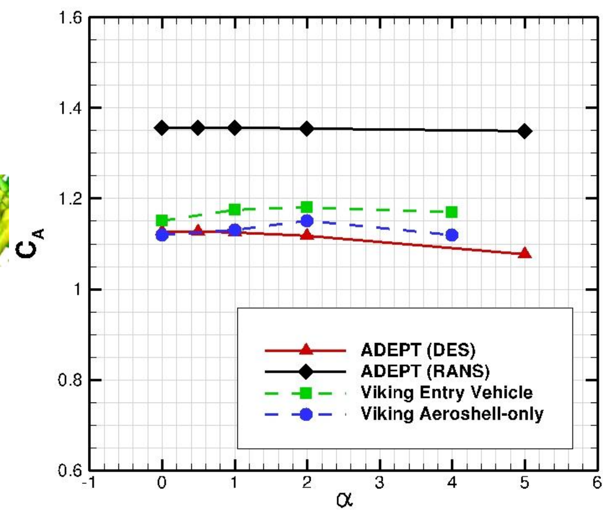

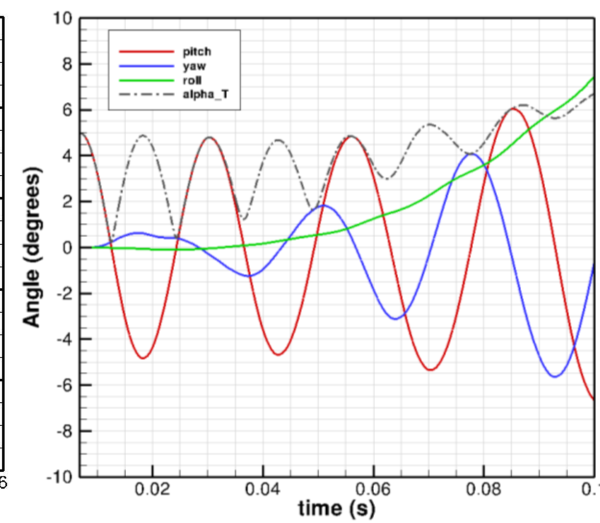

Pitch-Yaw Coupling: Divergence

Stern (AIAA-2012-3225)

Simulation of Injection and Mixing

90º injection in M=2 crossflow

Ethylene into air

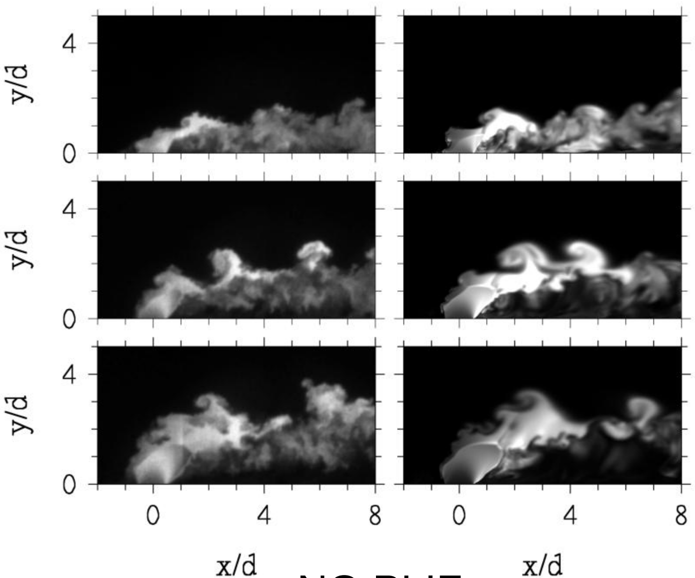

NO PLIF

Lin et. al

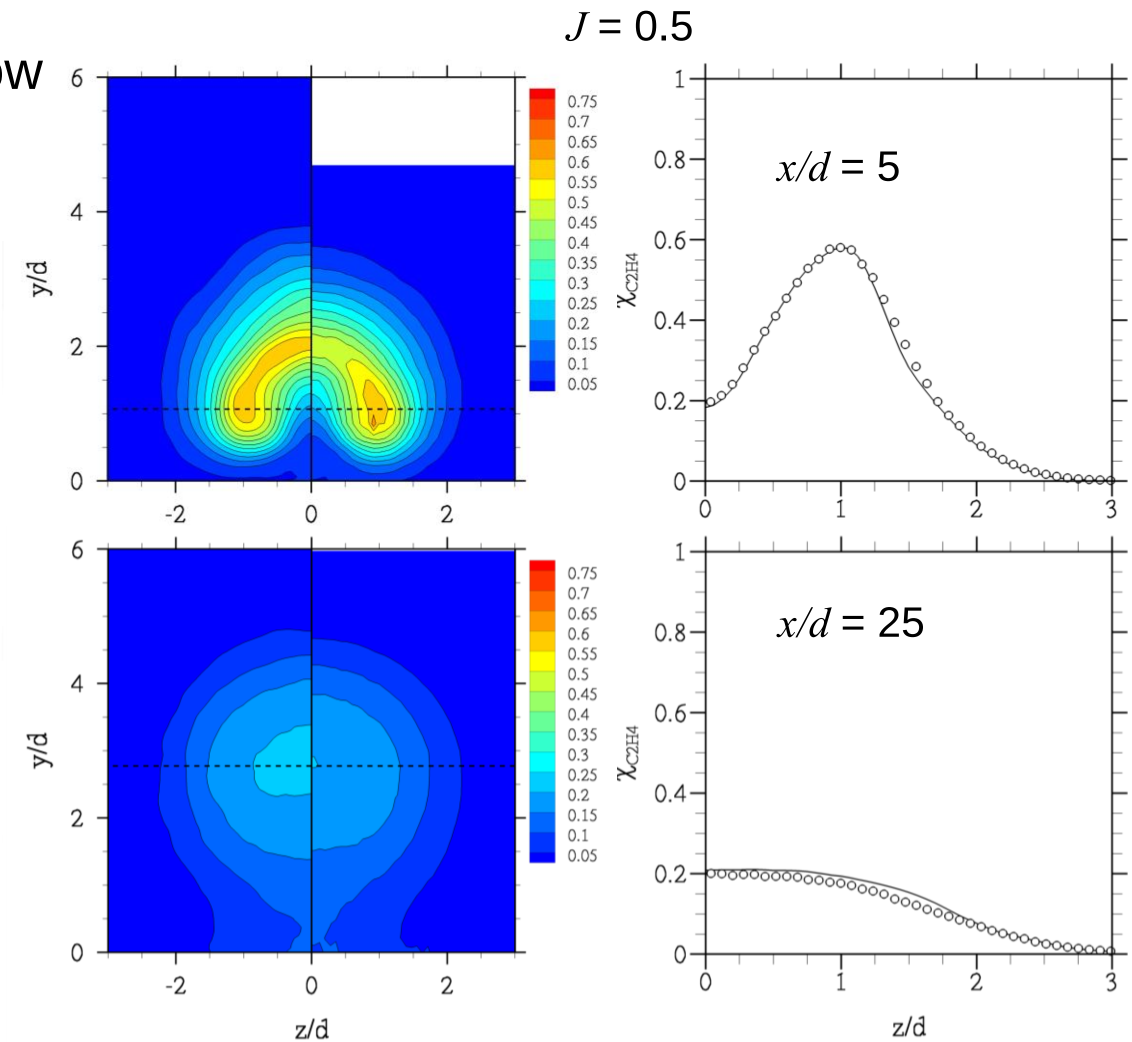

Mean injectant mole fraction measurements and simulation; data courtesy of C. Carter, AFRL

DNS of Mach 6 Turbulent Boundary Layer

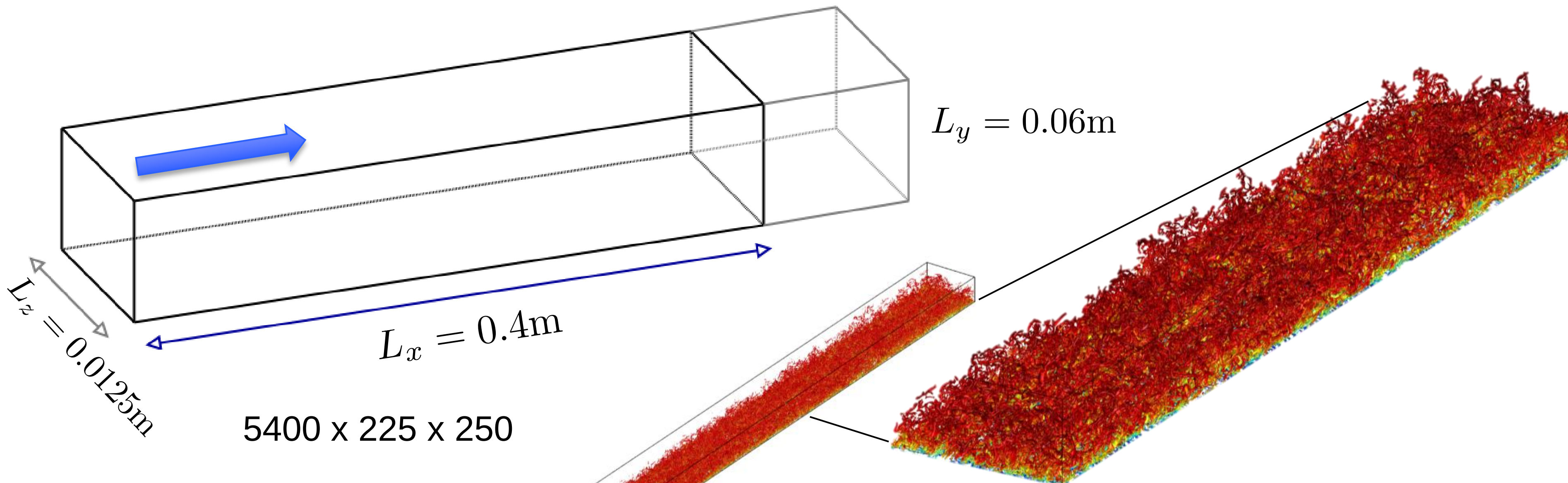

5400 x 225 x 250

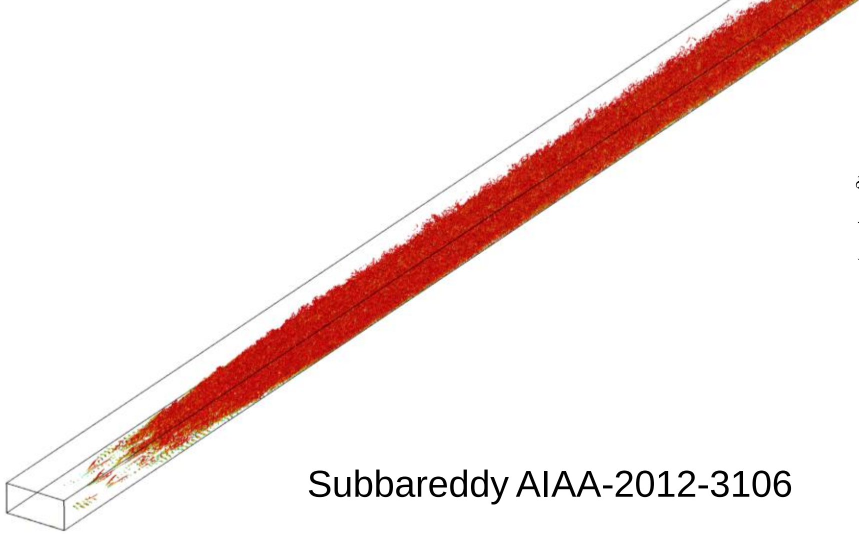

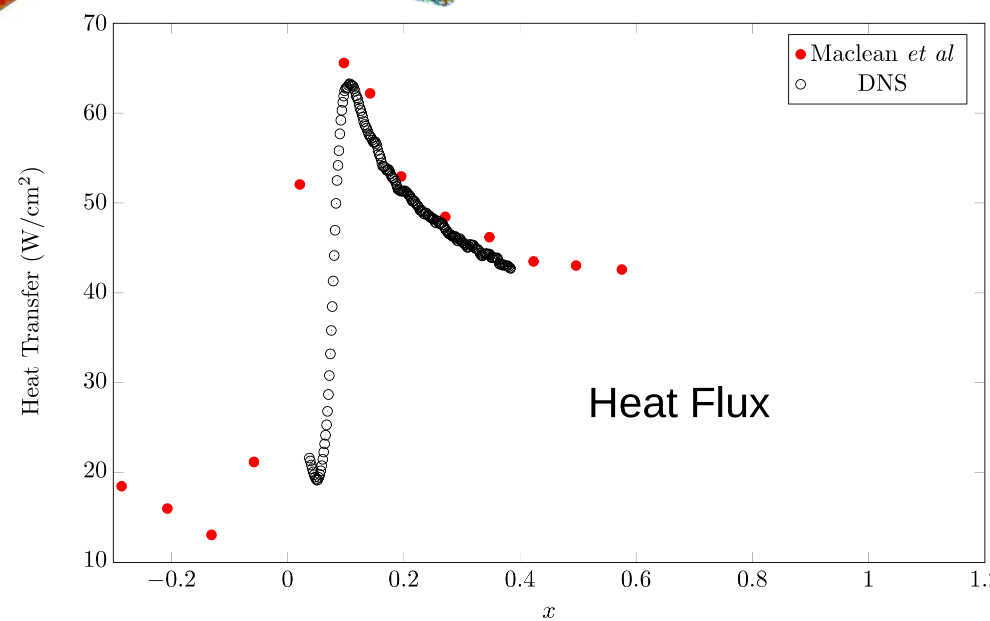

Subbareddy AIAA-2012-3106

Summary: In a Ten-Year Time Frame

- Scaling will be more of an issue: O(1T) elements
- Grid generation will remain painful
- Methods for data analysis will be needed
- Solutions will become less a function of the grid quality
- Much more complicated (accurate) physics models
- True multi-physics / multi-time scale simulations